ORIGINAL PAPER

Shear wave implications in wetting-induced collapse of sand–clay mixtures

Jongchan Kim[1] · Junghee Park[2] · Hyunwook Choo[3]

Abstract

Collapsible soils pose significant challenges to engineering projects due to their instability and sudden changes in volume upon variations in water content. In this study, the collapse potentials of specimens with sand–clay mixtures are experimentally investigated by considering factors, such as initial water content and clay fraction. The specimens are subjected to vertical stress up to $\sigma'_v = 440$ kPa in an instrumented oedometer cell, including the wetting process at $\sigma'_v = 220$ kPa. The settlement and shear wave velocity (V_s) are continuously measured during loading and wetting to propose a geophysical approach based on shear wave velocity measurements for better understanding of collapse mechanisms. The results show that the collapse potential of sand–clay mixtures increases with increasing clay fraction at a specific water content. However, the variation in the collapse potential can be the sole function of the clay water content (= water content/clay fraction). As the suction pressure decreases upon wetting, the V_s shows a time-dependent decrease during wetting, and the decreasing is proportional to the collapse potential, indicating the loss of small-strain stiffness. However, when the settlement ceases, a portion of V_s can be recovered over time because of the formation of a stable soil structure, leading to the ratio of V_s after collapse to V_s before collapse ranges from 0.85 to 1.05. Additionally, this study reveals that a relatively higher initial degree of saturation (> 50%) is necessary to recover stiffness/strength after soil collapse, emphasizing the importance of proper compaction in engineering projects involving collapsible soils.

Keywords Collapse potential · Sand–clay mixture · Clay water content · Shear wave velocity · Suction pressure

Introduction

Collapsible soils are a considerable concern in geotechnical engineering, posing risks to infrastructure and challenges for construction projects. These soils are widely distributed worldwide, covering 15–20% of Europe, China, and the United States, particularly in arid and semi-arid regions (Das 1995; Rogers 1995; Gao 1996; Gaaver 2012; Assadi-Langroudi et al. 2018). The collapse potential of sand-clay mixtures, which are common in natural deposits, has not been thoroughly investigated, despite its critical implications

for engineering applications. This study aims to bridge this knowledge gap by investigating the effects of initial water content, dry density, and clay content on the collapse potential of sand-clay mixtures, and by examining the relationship between collapse potential and shear wave velocity changes before and after the collapse.

Collapsible soils are characterized by their low density, low water content, and high sensitivity to changes in moisture content (Mitchell and Soga 2005; Roger 1995). Their unique structure, often described as a loose honeycomb-type arrangement, makes them susceptible to sudden volume changes (i.e., collapse) upon wetting, leading to catastrophic consequences such as landslides, differential settlement of structures, and instability of earthworks (Clemence and Finbarr 1981; Rollins and Rogers 1994). This instability typically arises from the breakdown of capillary suction pressure and cementation effects between particles when water content increases (Feda 1966; Lawton et al. 1989; Houston et al. 2001; Rao and Revanasiddappa 2002; Pereira et al. 2005). The collapse potential (C_p) is defined as the ratio

✉ Hyunwook Choo
    choohw@hanyang.ac.kr

[1] Civil Engineering, Department of Sustainable Engineering, Pukyong National University, Busan 48513, South Korea

[2] Department of Civil and Environmental Engineering, Incheon National University, Incheon 22012, South Korea

[3] Department of Civil and Environmental Engineering, Hanyang University, Seoul 04763, South Korea

between the change in height upon wetting (ΔH_w) and the initial specimen height (H_i), providing a quantitative measure of the volumetric change potential (ASTM D5333-03—ASTM 2003).

Natural soils can be highly complex in their composition; thus, natural coarse-grained sediments generally contain varying amounts of fines (particle size < 0.075 mm per Unified Soil Classification System, USCS) that can be categorized into silt or clay in geotechnical engineering (Monkul and Ozden 2007; Karakan and Demir 2018). Previous research has primarily focused on the impact of fine fractions on the behavior of coarse grains, examining aspects such as compressional and compaction behavior, undrained shear strength, and physical properties (e.g., Monkul and Ozden 2007; Cabalar and Hasan 2013; Cabalar and Mustafa 2017; Karakan and Demir 2018; Cabalar et al. 2020; Karakan et al. 2020; Kim et al. 2021; Shimobe et al. 2021). However, the effect of clay content on the collapse potential of sand or coarse-grained soils remains unclear. Furthermore, while previous studies have explored the volume changes associated with collapse (Mahmood and Abrahim 2021), the variations in mechanical properties, such as shear wave velocity, during this process have not been thoroughly investigated. Because the shear wave velocity is determined by interparticle contacts (determined by the applied stress) and interparticle coordination (determined by the packing state), shear wave velocity measurements for collapsible soils would be beneficial in terms of monitoring the decrease in capillary suction pressure during the collapse and the formation of a stable soil structure after the collapse.

Traditionally, the study of collapsible soils has been categorized into three approaches: (1) traditional (soil properties) approach, (2) microstructure (soil fabric) approach, and (3) soil mechanics-based approach (Li et al. 2016). Firstly, previous traditional approach has emphasized the soil property factors that influence collapse mechanisms, such as the dry density, Atterberg limits, initial water content, and clay content, and a large number of empirical equations have been proposed (Clevenger 1958; Gibbs and Bara 1962; Feda 1966; Li et al. 2016; Khodabandeh et al. 2023). Secondly, the microstructure approach has interpreted the effects of particle fabric, pore formation and distribution, and the form of bonding materials between particles on the collapse behavior (Assallay et al. 1997; Derbyshire and Mellors 1988; Romero and Simms 2008). Many researchers have tried to understand the soil pore patterns and stability of bonding materials, but there is a certain limitation to clearly evaluate those microstructures for fine-grained, such as silt and clay (Gu et al. 2011). Additionally, soil collapse is caused by multiple combinations of factors rather than one single reason because the soil properties primarily govern the microstructure of soils. Lastly, the soil mechanics-based approach has focused on the reduction of suction pressure among particles due to wetting, resulting in the significant volume change of collapsible soils (El-Ehwany and Houston 1990; Jotisankasa 2005; Pereira and Fredlund 2000). As mentioned above, the soil collapse is consequence of the complicated response among particles, which can be simultaneously affected by soil properties (approach 1), soil fabric (approach 2), and suction pressure (approach 3). Therefore, the main objective of this study is to evaluate the collapse potential of sand-clay mixture with various composition, and also to estimate the evolution of shear wave velocity (small-strain stiffness) before and after the collapse.

In this study, the effects of the initial water content, dry density, and clay content on the collapse potential of sand are investigated. To this end, silica sand specimens mixed with various clay fractions and water contents are consolidated in an oedometer cell and immersed in water to trigger collapse. The collapse potential is determined from the volume changes during the wetting process to estimate the significance of these factors. Additionally, the shear wave velocities before and after wetting are measured to correlate the changes in the small-strain stiffness and collapse potential. The correlations between collapse potential and small-strain stiffness can provide a better understanding of the geophysical manner of soil collapse, including the fabric alteration and stiffness recovery processes after the collapse. Furthermore, this study provides a new category for the study of collapse mechanism, which is geophysical approach, in additional to previous traditional, microstructure, and soil mechanics-based approaches.

Experimental study

Experimental device

In Fig. 1a, an instrumented oedometer cell is designed to measure the vertical displacement and shear wave velocity during the consolidation and wetting processes. The oedometer cell is made of stainless steel and has an inner diameter of 100 mm and a wall thickness of 10 mm to ensure K_0 consolidation conditions (i.e., negligible horizontal strain ($< 10^{-5}$)) during vertical loading. The top and bottom caps are equipped with a pair of bender elements (BE) to measure the shear wave velocities at various stress conditions, including wetting-induced soil collapse. The step input signal is generated from a function generator (Keysight 33210A) with a voltage of 10 V and a frequency of 20 Hz. Note, a step signal includes all frequencies; thus, a clear signal can be obtained regardless of soil stiffness (Lee and Santamarina 2005). The generated waves from the bottom bender element travel the specimen upwardly and are then captured at the top bender element. The captured signatures are averaged by stacking 1024 signals and displayed on an oscilloscope
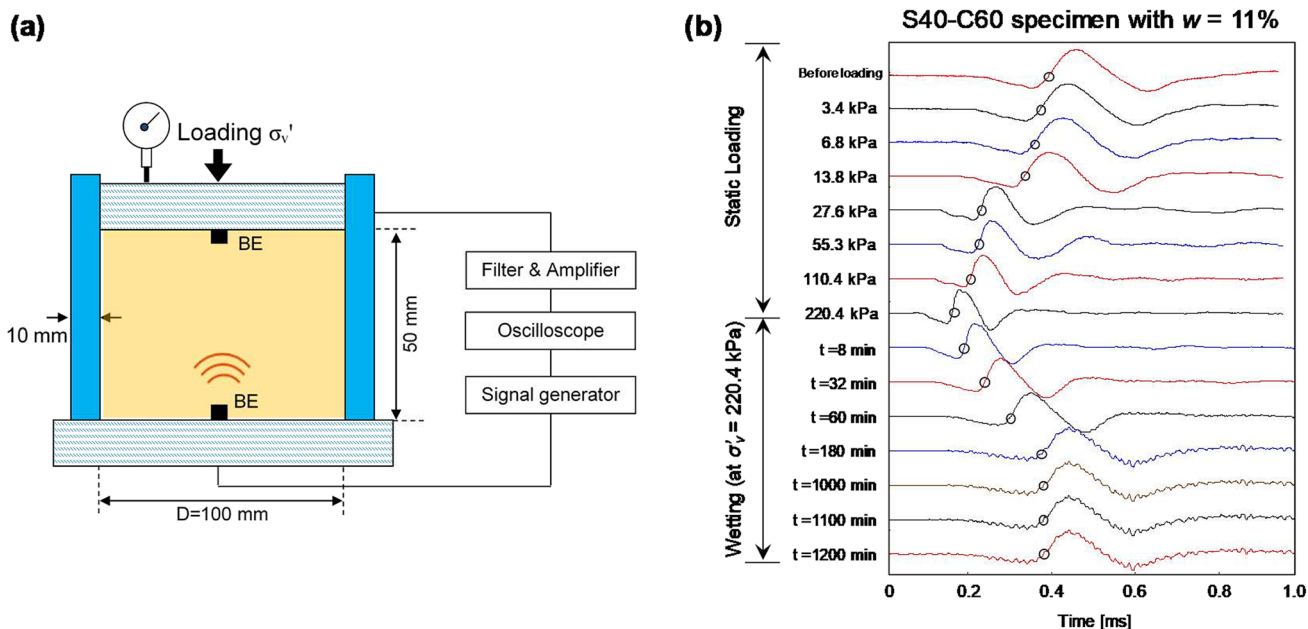
Fig. 1 (**a**) Schematic drawing of an instrumented oedometer cell and (**b**) typical shear wave signatures captured during the vertical loading and following wetting processes of S40-C60 specimen with water content (w) = 11%. Note the circles in figure (**b**) indicate the first arrival time

(Keysight DSOX 2014A) (Fig. 1b). The first arrival time (travel time) of the shear wave is determined according to recommendation of Lee and Santamarina (2005). The vertical displacement during loading and wetting is monitored using a linear variable differential transformer (LVDT), and updated specimen height is used to calculate the travel length of shear wave signatures.

Tested materials

The specimens are reconstituted using a mixture of silica sand and kaolin clay to imitate collapse-susceptible soils in the laboratory. Note silica sand is the most abundant type of sand found worldwide and kaolin clay is a very common clay type due to the abundance of kaolinite, which makes up the majority of its composition. The grain size distribution curves for the two unmixed soils are shown in Fig. 2. The soil index properties of the silica sand (K-5 sand, manufactured by Kyung In Material, South Korea) are as follows: coefficient of uniformity $C_u = 1.47$, median grain size $D_{50} = 800$ μm, specific surface $S_s = 0.03$ m^2/g, and specific gravity $G_s = 2.65$. Kaolin clay is manufactured by the Lakwoo Company, South Korea and has $D_{50} = 3.96$ μm, liquid limit $LL = 38.4\%$, plastic limit $PL = 23.6\%$, $S_s = 10.92$ m^2/g, and $G_s = 2.53$. Thus, according to the USCS, the tested sand and clay are classified as poorly graded sand (SP) and low-plasticity clay (CL), respectively. Sand–clay mixtures are prepared using predetermined sand/clay mass fractions, that
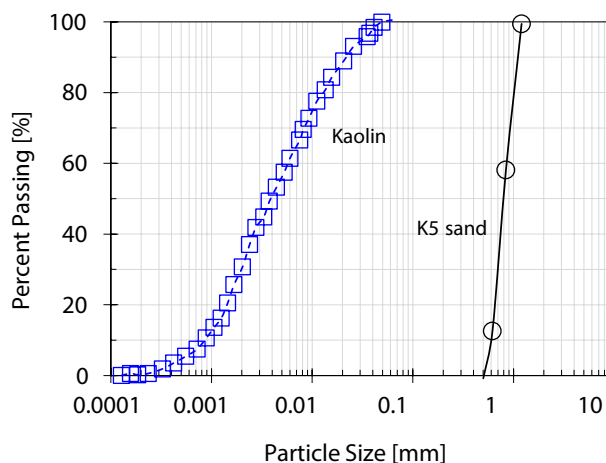

Fig. 2 Grain size distribution of the tested unmixed soils

is, S80-C20 (80% sand + 20% clay), S60-C40, S40-C60, and S20-C80.

Specimen preparation and experimental procedures

Modified proctor compaction tests are first performed to determine the variation in the dry unit weight according to the initial water content, as shown in Fig. 3 (ASTM D1557-12; ASTM 2012). The specimens are prepared with predetermined sand/clay mass fractions (i.e., S80-C20, S60-C40, S40-C60, and S20-C80) to evaluate the effects
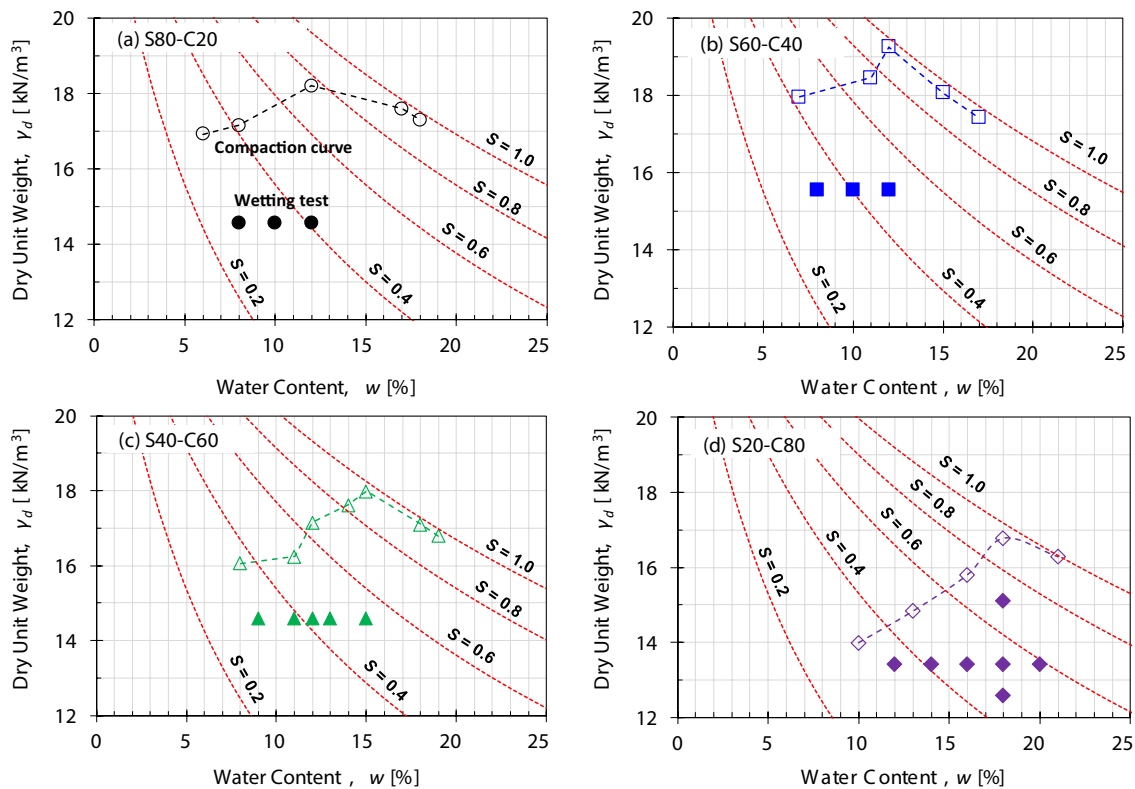
Fig. 3 Comparison of the compaction curve (empty markers with dotted line) and test conditions of the specimens (filled markers): (**a**) S80-C20 (i.e., specimens with sand fraction = 80% and clay fraction = 20%); (**b**) S60-C40; (**c**) S40-C60; (**d**) S20-C80 (note: S = degree of saturation)

of the clay fraction on the maximum dry unit weight and the corresponding optimum water content. The maximum dry unit weight and optimum water content of the mixtures varies with the sand/clay fraction: the S60-C40 specimens attain the highest maximum dry density at a water content of 12% (Fig. 3b), whereas the S20-C80 specimens exhibit the lowest maximum dry density at a water content of 18% (Fig. 3d). An increased optimum water content corresponds to an increased clay fraction. The results reveal that a larger amount of water is required to obtain the maximum dry unit weight with a higher clay fraction (Shimobe et al. 2021).

For the wetting tests, the sand–clay mixtures with predetermined initial water contents are premixed and stored in a plastic bag and placed in three layers in an oedometer cell. Tamping is performed to achieve the target dry unit weight. The initial water contents and dry unit weights of the tested specimens are shown in Fig. 3. The dry unit weight of the tested specimens is targeted to 80% of the maximum dry unit weight of each sand/clay fraction to represent the collapse-susceptible soil (i.e., non-compacted near-surface soil or insufficiently compacted soil with relatively lower relative compaction). Note that the soil collapse tends to be more pronounced in loose-packing soils. The specimens are prepared using various initial water contents to estimate the effects of the initial water content on the collapse potential.

Furthermore, complementary specimens (S20-C80) are tested at different dry unit weights at the optimum water content to evaluate the role of the packing density during the collapse.

The prepared specimens are subjected to stepwise vertical stress up to $\sigma'_v = 220$ kPa under K_0 consolidation conditions, after which they are inundated with distilled water for 24 h (ASTM D5333-03; ASTM 2003). An additional vertical stress of $\sigma'_v = 440$ kPa is then applied to the wet specimens to compare the compressibility before and after the collapse. Note that collapse index is generally measured at $\sigma'_v = 200$ kPa (per ASTM D5333). During these procedures, the vertical displacement is continuously monitored to assess the collapse potential triggered by wetting. Furthermore, shear wave signatures are continuously captured during the loading and wetting processes.

Results and discussion

Effect of inundation stress on collapse potential

This study measures the collapse potential at a vertical effective stress (inundation stress) of 220 kPa because of the predetermined oedometer cell size and set of weights

(note: the test protocol defines the collapse index as the collapse potential at inundation stress of 200 kPa [ASTM D5333]). Because the collapse potential varies with the magnitude of inundation stress (Howayek et al. 2011; Silveira and Rodrigues 2020), the collapse potentials of the S20-C80 samples (20% sand with 80% clay) with relative compaction of 80% and initial water content of 14% are measured at three inundation stress values (Fig. 4a). Figure 4b illustrates the effect of inundation stress on collapse potential (C_p), showing a slight increase in C_p with increasing vertical effective stress (σ'_v). The estimated C_p at $\sigma'_v = 200$ kPa, which is the collapse index, is approximately 8% based on interpolation, while the measured C_p at $\sigma'_v = 220$ kPa is 8.2% (Fig. 4b). This suggests that considering the measured collapse potential in this study as the collapse index would be practically acceptable.
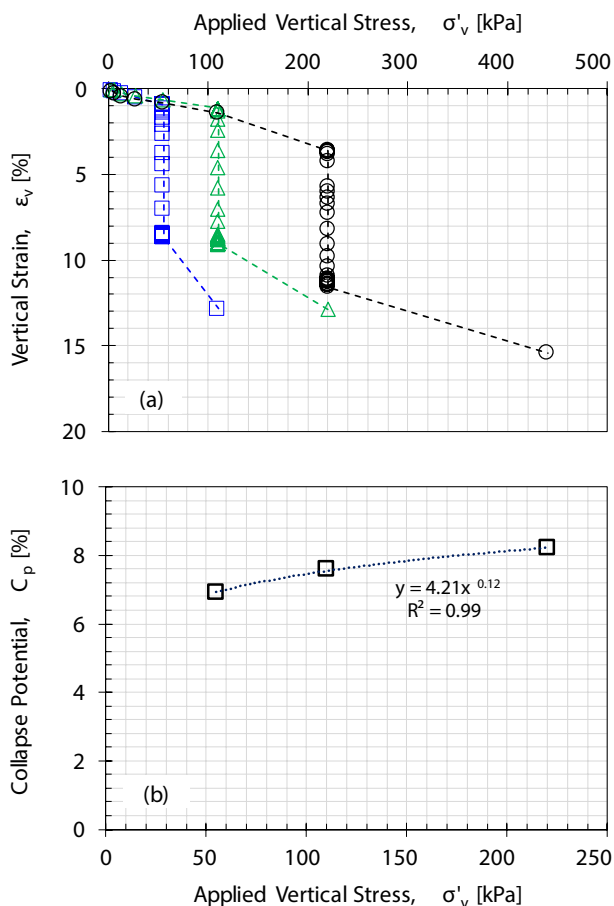

Fig. 4 Effect of inundation stress on collapse potential. (**a**) evolution of vertical strain of S20-C80 specimens with initial water content $w = 14\%$ during the K_0-consolidation and wetting at vertical stress of 55, 110, and 220 kPa; (**b**) variation of collapse potential according to inundation stress

Effect of initial water content on collapse potential

Figure 5 presents the relationship between the vertical (or volumetric) strain and the applied vertical stress (σ'_v) for the S40-C60 specimens (sand fraction = 40% and clay fraction = 60%) during the static loading history up to $\sigma'_v = 440$ kPa, where the wetting process occurs at $\sigma'_v = 220$ kPa. The vertical strain gradually increases until $\sigma'_v = 220$ kPa because of the compression of the voids (i.e., a decrease in the void ratio), followed by an abrupt change in the vertical strain during wetting at $\sigma'_v = 220$ kPa. This sharp volume reduction is mainly attributed to the wetting process, which disrupts the stability of the initial particle bonding at a specific initial water content. Soil stiffness under partially saturated conditions is primarily influenced by capillary pressure, which is a function of the water content and features of grain gradation (Wu et al. 1984; Cho and Santamarina 2001; Ng et al. 2020). Noticeably, S40-C60 specimens with higher initial water contents exhibit less significant volumetric changes when subjected to wetting under constant vertical stress.

Figure 6 shows the calculated collapse potentials of the tested specimens with various sand/clay fractions and a broad range of initial water contents. The results show that an increase in the initial water content decreases the collapse potential. Numerous previous studies have reported similar effects of water content on the collapse potential of soils because of the lower suction pressure at a higher water content (Li et al. 2016; Khodabandeh et al. 2023). Specifically, when the initial water content is lower than 2–4% below the optimum water content (w_{opt}), the effect of the water content on the variation in collapse potential is insignificant, although the measured collapse potential is large. In contrast, when the initial water content exceeds the values that are 2–4% lower than w_{opt} (dry of w_{opt}), the collapse potential rapidly decreases with increasing water content, and further reduction is expected in the wet of w_{opt} (i.e., higher water content than w_{opt}). The results indicate that the initial water content should be higher than 2–4% below the optimum water content (w_{opt}) to minimize the soil collapse potential (see similar observations in Howayek et al. 2011).

Effect of clay content on collapse potential

Figure 7 shows the evolution of the vertical strain in response to the vertical stress for the four specimens containing various sand/clay fractions at a fixed water content of 12%. Clearly, the collapse potential (C_p) at an identical initial water content of 12% tends to increase with increasing clay fraction. High capillary pressure builds up in clayey-dominant pores under unsaturated conditions, leading to enhanced soil stiffness (Agus et al. 2010); however, the suction-induced effective stress diminishes during the
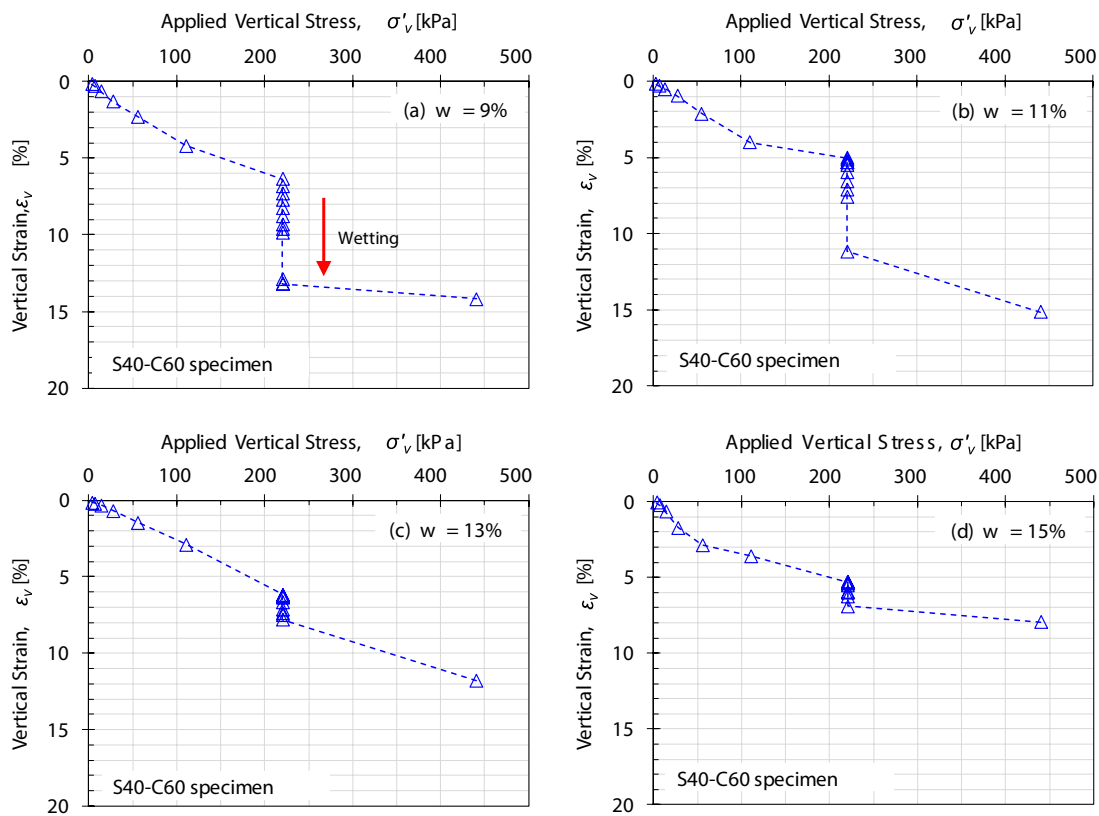
Fig. 5 Evolution of vertical strain of S40-C60 specimens during the K_0-consolidation and wetting. The wetting occurred at a vertical stress of 220 kPa, followed by an additional loading to 440 kPa. (**a**) Initial water content $w = 9\%$; (**b**) $w = 11\%$; (**c**) $w = 13\%$; (**d**) $w = 15\%$
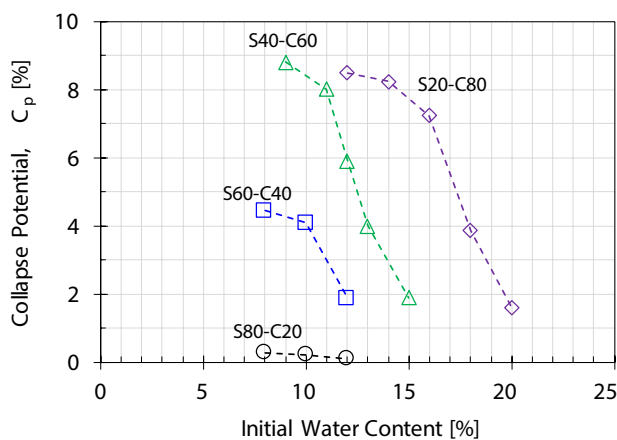

Fig. 6 Relationships between collapsible potential and initial water content

wetting process. Therefore, soil mixtures with higher clay fractions exhibit a more significant C_p during the wetting process. After wetting, the specimens with a higher clay fraction exhibit high volume compression during further static loading from $\sigma'_v = 220$ to $\sigma'_v = 440$ kPa, indicating the residual potential of soil deformation because of the higher

clay fraction (Choo et al. 2017). Note that the specimens with lower clay fractions (i.e., S80-C20 and S60-C40) show negligible changes in the compression index (C_c = change in void ratio/change in log σ'_v) before and after wetting, whereas the C_c values of specimens with higher clay fractions increases more than fivefold after collapse (Fig. 7), demonstrating that the specimens with higher clay fractions experience a more significant decrease in suction pressure than specimens with lower clay fractions.

Because the specific surface of kaolin particles is significantly larger than that of sand particles, it can be assumed that most of the water molecules are adsorbed by clay particles rather than sand particles at low water contents (Agus et al. 2010). Based on this assumption, the clay water content w_c (%) in Eq. (1) can capture the variation in suction pressure in sand–clay mixtures with varying water contents and clay fractions (f_c) (Agus et al. 2010).

$$w_c = \frac{w}{f_c} \tag{1}$$

where w = water content (weight ratio between water and solid, including sand and clay in this study); w_c, w, and f_c are in percentage. Figure 8 shows the collapse potential as a function of w_c and demonstrates that the collapse
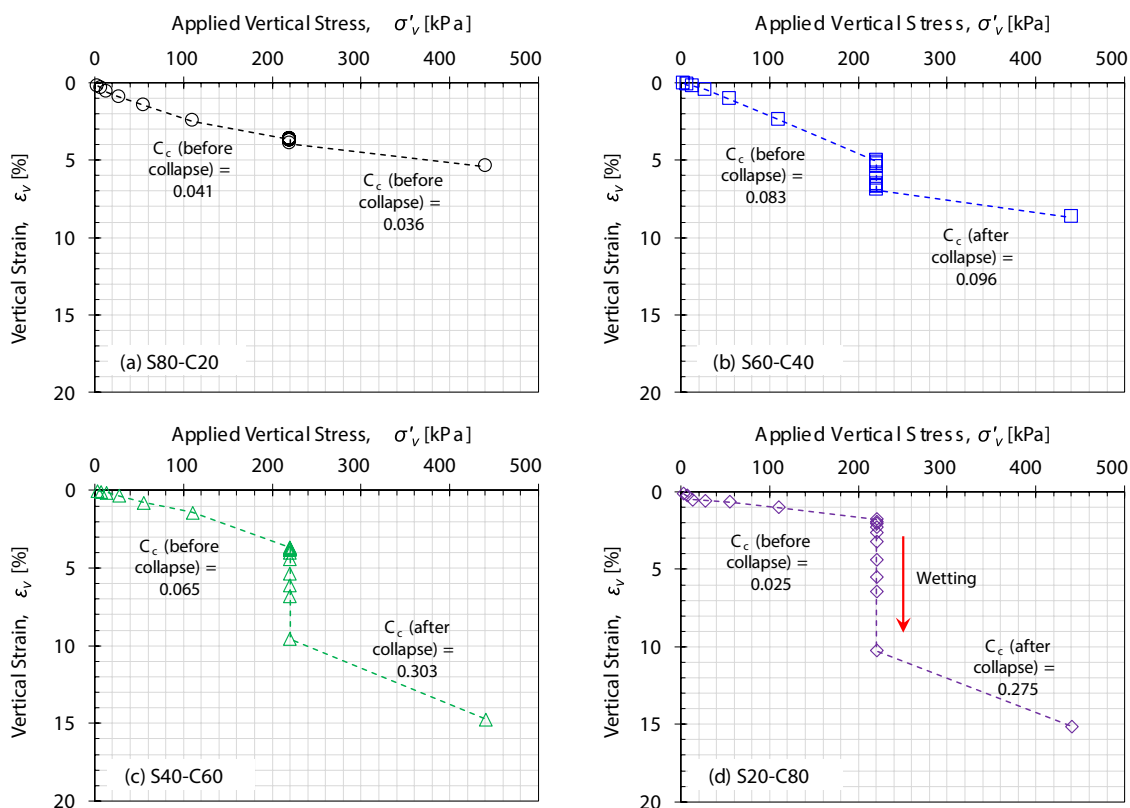
Fig. 7 Evolution of vertical strain during the K_0-consolidation and wetting under the identical initial water content $w = 12\%$: (**a**) S80-C20; (**b**) S60-C40; (**c**) S40-C60; (**d**) S20-C80
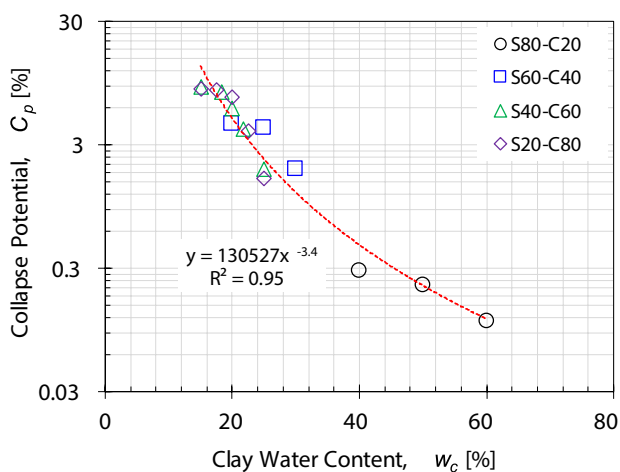

Fig. 8 Relationships between collapse potential and clay water content of the tested specimens with varying clay fractions. Note clay water content w_c = Eq. (1)

potential follows the power function of w_c. Surprisingly, the four curves of the collapse potential versus the initial water content space in Fig. 6 appear to merge into a single trend (Fig. 8). In other words, the variation in the collapse

potentials of the tested materials with varying clay fractions could be the sole function of w_c. Because w_c determines the suction pressure of sand–clay mixtures, Fig. 8 indicates that a decrease in soil suction is the most important reason for the collapse behavior of soils (Mahmood and Abrahim 2021).

Effect of dry unit weight on collapse potential

The tested specimens containing various sand/clay fractions have different ranges of dry unit weights, as shown in Fig. 3. Complementary tests are conducted on the S20-C80 specimens (i.e., sand fraction = 20% and clay fraction = 80%) at an initial water content of 18% (= optimum water content for the S20-C80 specimen) to clearly explore the effects of packing density on the collapse potential (Fig. 3d). Figure 9a shows that a higher dry unit weight constrains the collapse potential compared to a relatively lower dry unit weight because densely packed specimens tend to exhibit a greater frictional resistance. Additionally, a change in the dry unit weight at a constant water content results in a change in the degree of saturation. Because the degree of saturation is one of the most critical parameters that influence the collapse
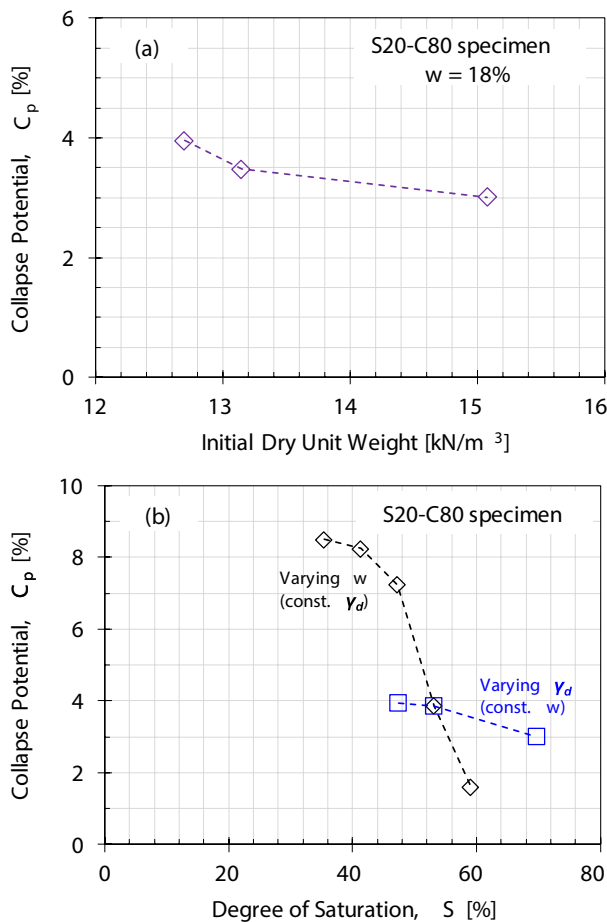
Fig. 9 Effects of (**a**) initial dry unit weight and (**b**) degree of saturation on the collapsible potential of S20-C80 specimens

potential (Basma and Tuncer 1992; Li et al. 2016; Hou et al. 2021; Khodabandeh et al. 2023), the collapse potential of the S20-C80 specimens is plotted as a function of the degree of saturation in Fig. 9b. For comparison, the results of the S20-C80 specimens with varying initial water contents in Fig. 6 also overlap in Fig. 9b. Because an increase in the dry unit weight results in a decrease in the degree of saturation and the consequent less contribution of the metastable forces supporting the soil particles prior to wetting, the collapse potential decreases with increasing dry unit weight. However, the changes in the collapse potential caused by the dry unit weight are less significant than those caused by the water content (Fig. 9b). This implies that the dry unit weight has a secondary effect on the collapse potential, particularly in specimens with a high collapse potential (i.e., S20-C80). In this context, it is notable that the total suction of sand–clay mixtures is mainly determined by the initial water content, whereas the influence of the initial dry density on the magnitude of the suction pressure is insignificant (Agus et al. 2010).

Shear wave velocity reduction during wetting

The shear wave velocity (V_s) is measured during the consolidation and wetting processes. Figure 10 shows the V_s evolution for the S40-C60 specimens with different initial water contents. Because the applied stress determines the interparticle contact stiffness, the V_s of dry and saturated soils can be expressed as a power function of the mean effective stress (σ'_m):

$$V_s = \alpha \cdot \left(\frac{\sigma_m'}{P_r} \right)^{\beta} \tag{2}$$

where α and β are experimentally determined fitting parameters and P_r is the reference pressure (= 1 kPa) in unit matching σ'_m. The α-factor corresponds to the V_s value at $\sigma'_m = P_r = 1$ kPa and significantly reflects the packing state (i.e., interparticle coordination), and the β-exponent corresponds to the V_s sensitivity of tested materials to the changes in σ'_m. In the case of unsaturated soils, the matric suction ($u_a - u_w$, where u_a is the pore air pressure, and u_w is the pore water pressure) gives an additional increase in interparticle contact stiffness (Kim et al. 2023; Shwan 2023). Note the osmotic suction is negligible in the case where the pore water is tap water or deionized water (Alramahi et al. 2010; Mahmood and Abrahim 2021). Thus, Eq. (2) can be modified as follows (Clariá and Rinaldi 2007):

$$V_s = \alpha \cdot \left(\frac{\sigma_m'}{P_r} \right)^{\beta} + \lambda \cdot \left(u_a - u_w \right) \tag{3}$$

where λ is the fitting parameter, which reflects the packing state and soil type.

During vertical loading (i.e., consolidation), an increasing trend in V_s is observed because of the improved soil stiffness at a higher vertical effective stress σ'_v (Eqs. (2) and (3), and Fig. 10). However, a sharp decrease in V_s occurs during wetting, mainly owing to the loss of soil stiffness at higher water contents. Additional loading of $\sigma'_v = 440$ kPa after wetting results in an increase in V_s (Eq. (2) and Fig. 10). As already implied in the comparison between Eqs. (2) and (3), this observation indicates that wetting-induced collapse prevails when a reduction in small-strain stiffness results from the breakage of the metastable soil fabric due to decreased soil suction. Similar to the results presented in Fig. 5, Fig. 10 also shows a significant decrease in the V_s values of the specimens with lower initial water contents, indicating that the specimens with higher volume compression (i.e., greater collapse potential) during the wetting process exhibit a greater reduction in V_s.

Figure 11 presents the relationship between the collapse potential and shear wave velocity reduction ΔV_s during wetting. The collapse of the specimens is triggered by
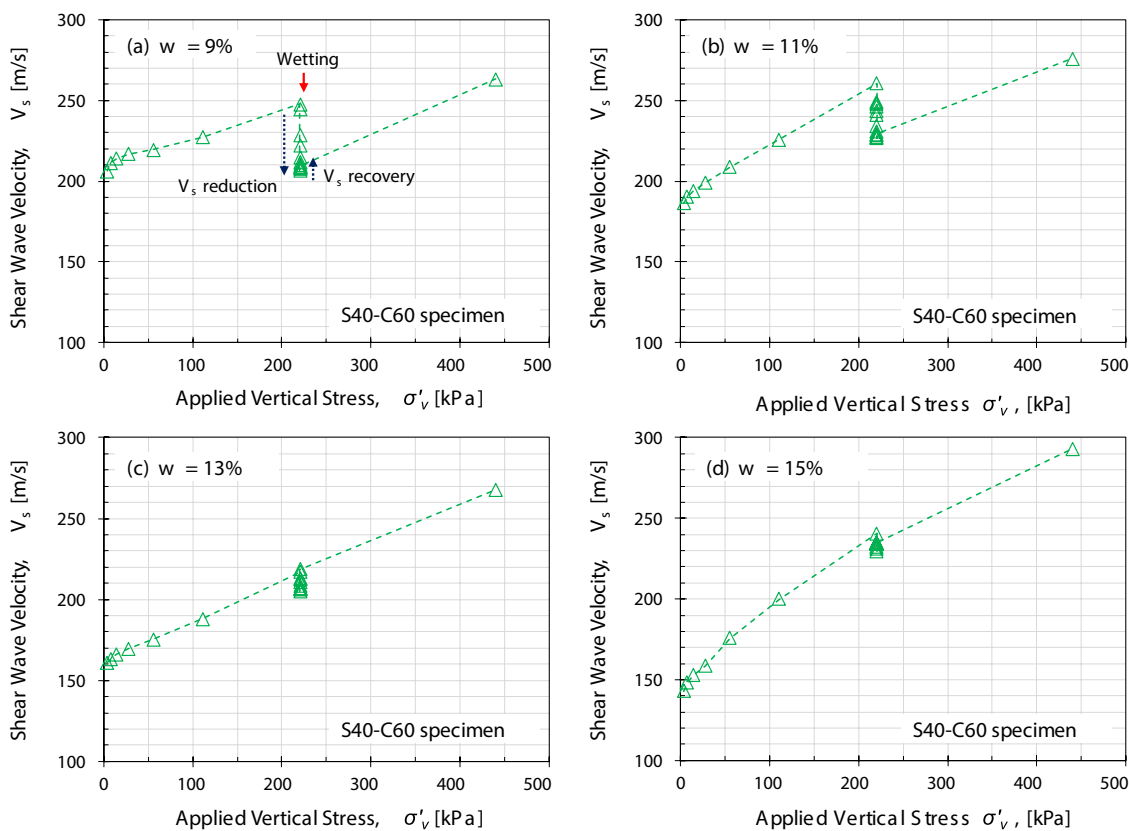
Fig. 10 Shear wave velocity values during the K_0-consolidation and wetting of S40-C60 specimens with different initial water content: (**a**) initial water content $w = 9\%$; (**b**) $w = 11\%$; (**c**) $w = 13\%$; (**d**) $w = 15\%$. The wetting occurred at a vertical stress of 220 kPa. The captured typical shear wave signatures are presented in Fig. 1
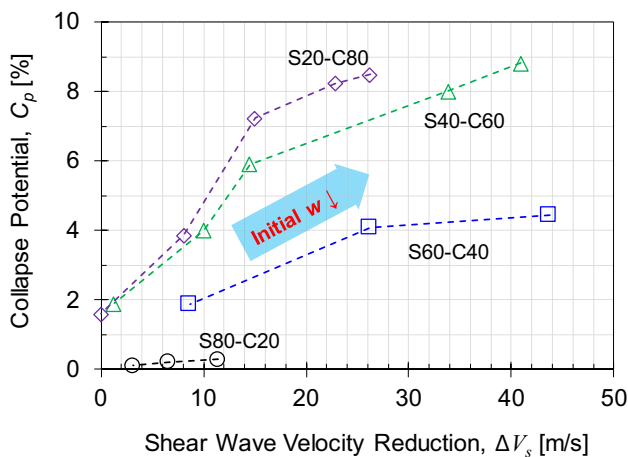

Fig. 11 Relationships between collapse potential and shear wave velocity reduction during wetting

the influence of decreased suction pressure on the collapse potential and ΔV_s differs according to the soil type. At the later part of the wetting, the measured V_s show an increased trend (recovery) with time, following the V_s reduction upon wetting (Fig. 10). More details of V_s recovery will be discussed in the next Section.

Sher wave velocity recovery during wetting

Soils often involve time-varying load–deformation responses; in fact, some portion of shear wave velocity (V_s) can be recovered during wetting (Fig. 10). Thus, Fig. 12a shows the time-dependent variations in the volumetric strain and V_s for the S60-C40 specimen at an initial water content of $w = 9\%$. Rearrangement of soil particles (or volume compression of soil) occurs when the induced stress in the soil exceeds the frictional resistance between the soil particles (Won et al. 2023). As the wetting process induces a decrease in suction pressure and a consequent decrease in effective stress as a function of time, the frictional resistance between the soil particles decreases during wetting processes. Thus, under a constant applied stress level (i.e., an inundation stress of 220 kPa), the tested specimens settle over time and
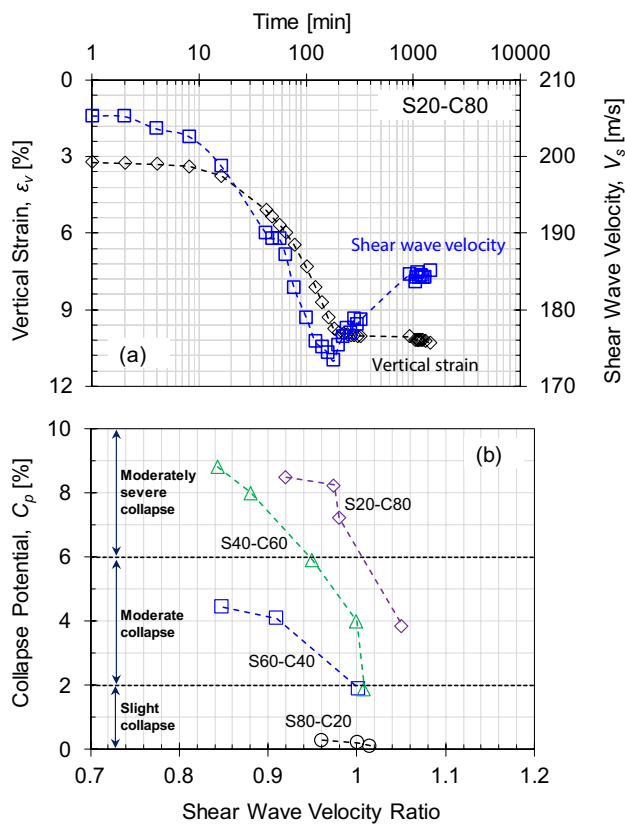
a reduction in stiffness, resulting in a greater reduction in V_s. This increases the collapse potential, leading to a positive relationship between ΔV_s and the collapse potential. Figure 11 also shows that ΔV_s increase with decreasing clay fraction at a given collapse potential. This implies that

Fig. 12 Shear wave velocity response during soil collapse: (a) time-dependent collapsible soil behavior, including the variations of vertical strain and shear wave velocity of S20-C80 specimen with initial water content $w = 14\%$; (b) relationships between collapse potential and shear wave velocity ratio. Note shear wave velocity ratio = shear wave velocity after collapse / shear wave velocity before collapse

The shear wave velocity ratio (V_s ratio = V_s after collapse / V_s before collapse) is defined, and a relationship of the collapse potential against the V_s ratio is plotted to quantify the degree of shear wave velocity recovery (Fig. 12b). The V_s ratio increases with decreasing collapse potential. This observation indicates that V_s with higher initial water contents in the soil exhibited lower dependency on suction stress; therefore, the decreased V_s induced by the loss of soil suction could be recovered by forming a new stable soil structure. In addition, soils with a moderate degree of collapse, according to ASTM D5333, can exhibit a V_s ratio of 0.85, indicating that moderately collapsible soils can exhibit a 15% decrease in V_s upon wetting (Fig. 12b). Note that a 15% decrease in V_s indicates a decrease of 28% in the small-strain stiffness. Thus, the collapse of soils affects both the serviceability and stability of geostructures. Although the settlement ceases after the wetting-induced collapse and a higher dry density is expected, the initial stiffness (or mechanical properties) could not be recovered (Fig. 10).

The V_s ratio of the tested materials is plotted as a function of the initial degree of saturation (S) to determine the condition where V_s could be fully recovered after the collapse because the tested materials showed different optimum water contents and maximum dry unit weights according to the clay fractions (Fig. 13). Most notably, it can be observed that the V_s ratios of all tested materials with varying clay fractions and initial water contents are equal to or greater than 1.0 when the nominal S is greater than approximately 50%. Thus, being apart from the settlement of collapsible soils, the sand–clay mixtures used in the compaction fill should be compacted to have an initial degree of saturation exceeding 50% to prevent permanent stiffness/strength loss upon wetting.

reach a stable volumetric state and asymptotic strain. Similarly, a progressive decrease in V_s with time is observed upon wetting, as shown in Fig. 12a. However, V_s slightly increase after ~200 min when settlement ceases, reflecting the emergence of a new stable soil structure.

The second term in Eq. (3) decreases upon wetting, resulting in a time-dependent decrease in V_s during wetting. However, the collapse of soils (i.e., a large volume decrease in soils) results in the rearrangement of soil particles to achieve a dense packing condition (i.e., increased interparticle coordination). Thus, the α-factor in Eq. (2) after collapse is greater than that in Eq. (3) before collapse, resulting in some recovery of V_s. Many previous studies reported that stiff materials exhibit greater α, and the α value for a given soil increases with decreasing void ratio (Santamarina et al. 2001; Choo and Burns 2015; Won et al. 2023). This V_s recovery during wetting can also be attributed to the increase in mean effective stress (Eq. 2) because the horizontal stress under the constant σ'_v increases upon wetting (Fattah and Dawood 2020; Mahmood and Abrahim 2021).

Conclusions

In this study, the collapse potentials of specimens with various sand–clay fractions are experimentally investigated by considering factors, such as the initial water and clay content. The specimens are subjected to a static vertical stress up to $\sigma'_v = 440$ kPa in an instrumented oedometer cell, where they experience wetting at a constant $\sigma'_v = 220$ kPa. The shear wave velocity (V_s) is continuously measured during the loading and wetting processes. The main findings are summarized as follows.

- The calculated collapse potentials of the tested specimens containing various sand/clay fractions decrease with increasing initial water content and dry unit weight because of the less significant contribution of the metastable forces supporting the soil particles before wetting.
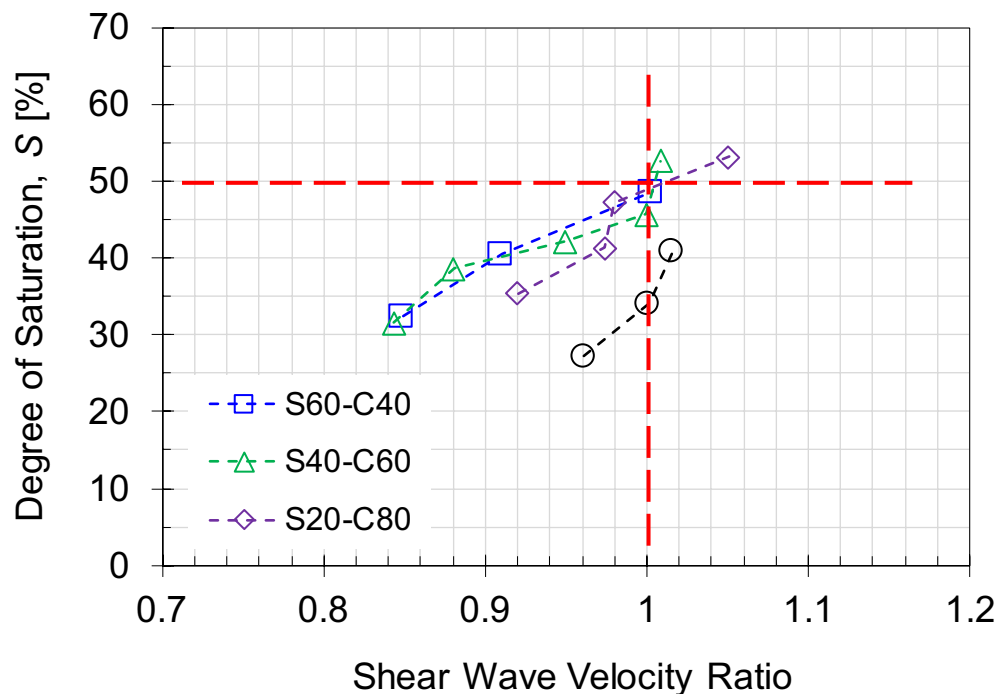
Fig. 13 Relationship between initial degree of saturation and shear wave velocity ratio

- The collapse potential of the tested sand–clay mixtures increases with increasing clay fraction at a specific water content. However, the variation in the collapse potential of the tested materials with varying clay fractions and water contents is the sole function of the clay water content regardless of the clay fraction because most of the water molecules are adsorbed by clay particles.

- Because the suction pressure fades away during the wetting process, the shear wave velocity (V_s) of the tested materials shows a time-dependent decrease during wetting. However, when the settlement ceases, a portion of the shear wave velocity could be recovered over time because of forming a new stable soil structure with a denser packing state and greater lateral effective stress. This results in that the ratio of V_s before collapse to V_s after collapse ranges from 0.85 to 1.05.

- Shear wave velocity measurements successfully capture the loss of capillary suction pressure (i.e., small-strain stiffness) during the wetting. More pronounced collapse potential and shear wave velocity reduction are observed with the decrease in the initial water content.

- Similar time-dependent variations of shear wave velocity and settlement during wetting, and the positive relationship between shear wave velocity reduction and collapse potential imply that the geophysical approach, newly suggested in this study based on shear wave velocity measurements, can be beneficially employed as a tool for the study of collapse mechanism.

- The decrease in the shear wave velocity upon wetting could be fully recovered when the initial degree of saturation of the tested materials is greater than approximately 50%. Therefore, it is suggested that the initial degree of saturation should be higher than 50% in the compaction fill to expect the recovery of stiffness/strength after the soil collapse behavior.

References

Agus SS, Schanz T, Fredlund DG (2010) Measurements of suction versus water content for bentonite–sand mixtures. Can Geotech J 47(5):583–594. https://doi.org/10.1139/t09-120

Alramahi B, Alshibli KA, Fratta D (2010) Effect of fine particle migration on the small-strain stiffness of unsaturated soils. J Geotech Geoenviron Eng 136(4):620–628. https://doi.org/10.1061/(asce)gt.1943-5606.0000244

Assadi-Langroudi A, Ng'ambi S, Smalley I (2018) Loess as a collapsible soil: Some basic particle packing aspects. Quatern Int 469:20–29. https://doi.org/10.1016/j.quaint.2016.09.058

Assallay AM, Rogers CDF, Smalley IJ (1997) Formation and collapse of metastable particle packings and open structures in loess

deposits. Eng Geol 48(1–2):101–115. https://doi.org/10.1016/s0013-7952(97)81916-3

ASTM (2003) Standard Test Methods for Measurements of Collapse Potential of Soils, ASTM D5333–03. ASTM, West Conshohochen, PA. https://doi.org/10.1520/d5333-03

ASTM (2012) Standard Test Methods for Laboratory Compaction Characteristics of Soil Using Modified Effort (56,000 ft-lbf/ft3 (2,700 kN-m/m3)), ASTM D1557–12. ASTM, West Conshohochen, PA. https://doi.org/10.1520/d1557-02e01

Basma AA, Tuncer ER (1992) Evaluation and control of collapsible soils. J Geotech Eng 118(10):1491–1504. https://doi.org/10.1061/(asce)0733-9410(1992)118:10(1491)

Cabalar AF, Hasan RA (2013) Compressional behaviour of various size/shape sand–clay mixtures with different pore fluids. Eng Geol 164:36–49. https://doi.org/10.1016/j.enggeo.2013.06.011

Cabalar AF, Mustafa WS (2017) Behaviour of sand–clay mixtures for road pavement subgrade. Int J Pavement Eng 18(8):714–726. https://doi.org/10.1080/10298436.2015.1121782

Cabalar AF, Khalaf MM, Isik H (2020) A comparative study on the undrained shear strength results of fall cone and vane shear tests in sand–clay mixtures. Arab J Geosci 13:1–11. https://doi.org/10.1007/s12517-020-05351-5

Cho GC, Santamarina JC (2001) Unsaturated particulate materials - Particle-level studies. J Geotech Geoenviron Eng 127(1):84–96. https://doi.org/10.1061/(asce)1090-0241(2001)127:1(84)

Choo H, Burns SE (2015) Shear wave velocity of granular mixtures of silica particles as a function of finer fraction, size ratios and void ratios. Granular Matter 17:567–578. https://doi.org/10.1007/s10035-015-0580-2

Choo H, Lee W, Lee C (2017) Compressibility and small strain stiffness of kaolin clay mixed with varying amounts of sand. KSCE J Civ Eng 21:2152–2161. https://doi.org/10.1007/s12205-016-1787-4

Clariá J, Rinaldi V (2007) Shear wave velocity of a compacted clayey silt. Geotech Test J 30(5):399–408. https://doi.org/10.1520/gtj100655

Clemence SP, Finbarr AO (1981) Design considerations for collapsible soils. J Geotech Eng Div 107(3):305–317. https://doi.org/10.1061/ajgeb6.0001102

Clevenger WA (1958) Experiences with loess as foundation material. Trans Am Soc Civ Eng 123(1):151–169. https://doi.org/10.1061/taceat.0007546

Das B (1995) Principles of foundation engineering. PWS Publ Co, Boston

Derbyshire E, Mellors TW (1988) Geological and geotechnical characteristics of some loess and loessic soils from China and Britain: a comparison. Eng Geol 25(2–4):135–175. https://doi.org/10.1016/0013-7952(88)90024-5

El-Ehwany M, Houston SL (1990) Settlement and moisture movement in collapsible soils. Journal of Geotechnical Engineering 116(10):1521–1535. https://doi.org/10.1061/(asce)0733-9410(1990)116:10(1521)

Fattah MY, Dawood BA (2020) Time-dependent collapse potential of unsaturated collapsible gypseous soils. World Journal of Engineering 17(2):283–294. https://doi.org/10.1108/wje-09-2019-0276

Feda J (1966) Structural stability of subsident loess soil from Praha-Dejvice. Eng Geol 1(3):201–219. https://doi.org/10.1016/0013-7952(66)90032-9

Gaaver KE (2012) Geotechnical properties of Egyptian collapsible soils. Alex Eng J 51(3):205–210. https://doi.org/10.1016/j.aej.2012.05.002

Gao G (1996) The distribution and geotechnical properties of loess soils, lateritic soils and clayey soils in China. Eng Geol 42(1):95–104. https://doi.org/10.1016/0013-7952(95)00056-9

Gibbs H, Bara J (1962) Predicting surface subsidence from basic soil tests, in Field Testing of Soils, edited. ASTM International. https://doi.org/10.1520/stp47043s

Gu TF, Wang JD, Guo L, Wu DL, Li KC (2011) Study of Q3 loess microstructure changes based on image processing. Chin J Rock Mech Eng 30(S1):3185–3192

Hou Y, Li P, Wang J (2021) Review of chemical stabilizing agents for improving the physical and mechanical properties of loess. Bull Eng Geol Env 80:9201–9215. https://doi.org/10.1007/s10064-021-02486-x

Houston SL, Houston WN, Zapata CE, Lawrence C (2001) Geotechnical engineering practice for collapsible soils. Geotech Geol Eng 19(3):333–355. https://doi.org/10.1007/978-94-015-9775-3_6

Howayek AE, Huang PT, Bisnett R, Santagata MC (2011) Identification and behavior of collapsible soils (No. FHWA/IN/JTRP-2011/12). Purdue University: Joint Transportation Research Program. https://doi.org/10.5703/1288284314625

Jotisankasa A (2005) Collapse behaviour of a compacted silty clay. Doctoral dissertation, University of London

Karakan E, Demir S (2018) Effect of fines content and plasticity on undrained shear strength of quartz-clay mixtures. Arab J Geosci 11:1–12. https://doi.org/10.1007/s12517-018-4114-1

Karakan E, Shimobe S, Sezer A (2020) Effect of clay fraction and mineralogy on fall cone results of clay–sand mixtures. Eng Geol 279:105887. https://doi.org/10.1016/j.enggeo.2020.105887

Khodabandeh MA, Nagy G, Török Á (2023) Stabilization of collapsible soils with nanomaterials, fibers, polymers, industrial waste, and microbes: Current trends. Constr Build Mater 368:130463. https://doi.org/10.1016/j.conbuildmat.2023.130463

Kim SY, Park J, Lee JS (2021) Coarse-fine mixtures subjected to repetitive Ko loading: Effects of fines fraction, particle shape, and size ratio. Powder Technol 377:575–584. https://doi.org/10.1016/j.powtec.2020.09.017

Kim M, Lee C, Kim JU, Choo H (2023) Use of shear wave velocity for assessing engineering properties of compacted bentonite after swelling. Sci Rep 13(1):15705. https://doi.org/10.1038/s41598-023-42779-7

Lawton EC, Fragaszy RJ, Hardcastle JH (1989) Collapse of compacted clayey sand. J Geotech Eng 115(9):1252–1267. https://doi.org/10.1061/(asce)0733-9410(1989)115:9(1252)

Lee JS, Santamarina JC (2005) Bender elements: performance and signal interpretation. J Geotech Geoenviron Eng 131(9):1063–1070. https://doi.org/10.1061/(asce)1090-0241(2005)131:9(1063)

Li P, Vanapalli S, Li T (2016) Review of collapse triggering mechanism of collapsible soils due to wetting. J Rock Mech Geotech Eng 8(2):256–274. https://doi.org/10.1016/j.jrmge.2015.12.002

Mahmood MS, Abrahim MJ (2021) A review of collapsible soils behavior and prediction. IOP Conf Ser Mater Sci Eng 1094(1):012044. https://doi.org/10.1088/1757-899x/1094/1/012044

Mitchell JK, Soga K (2005) Fundamentals of soil behavior. Wiley, New York

Monkul MM, Ozden G (2007) Compressional behavior of clayey sand and transition fines content. Eng Geol 89(3–4):195–205. https://doi.org/10.1016/j.enggeo.2006.10.001

Ng CWW, Zhou C, Chiu CF (2020) Constitutive modelling of state-dependent behaviour of unsaturated soils: an overview. Acta Geotech 15:2705–2725. https://doi.org/10.1007/s11440-020-01014-7

Pereira JH, Fredlund DG (2000) Volume change behavior of collapsible compacted gneiss soil. J Geotech Geoenviron Eng 126(10):907–916. https://doi.org/10.1061/(asce)1090-0241(2000)126:10(907)

Pereira JH, Fredlund DG, CardãoNeto MP, Gitirana GDF Jr (2005) Hydraulic behavior of collapsible compacted gneiss soil. J Geotech Geoenviron Eng 131(10):1264–1273. https://doi.org/10.1061/(asce)1090-0241(2005)131:10(1264)

Rao S, Revanasiddappa K (2002) Collapse behaviour of a residual soil. Géotechnique 52(4):259–268. https://doi.org/10.1680/geot.52.4.259.41025

Rogers C (1995) Types and distribution of collapsible soils, Genesis and properties of collapsible soils. In: NATO ASI series, vol. 468. Kluwer Academic Publishers, Dordrecht, pp 1–17. https://doi.org/10.1007/978-94-011-0097-7_1

Rollins KM, Rogers GW (1994) Mitigation measures for small structures on collapsible alluvial soils. J Geotech Eng 120(9):1533–1553. https://doi.org/10.1061/(asce)0733-9410(1994)120:9(1533)

Romero E, Simms PH (2008) Microstructure investigation in unsaturated soils: a review with special attention to contribution of mercury intrusion porosimetry and environmental scanning electron microscopy. Geotech Geol Eng 26:705–727. https://doi.org/10.1007/978-1-4020-8819-3_8

Santamarina JC, Klein A, Fam MA (2001) Soils and waves: Particulate materials behavior, characterization and process monitoring. J Soils Sediments 1(2):130–130. https://doi.org/10.1007/bf02987719

Shimobe S, Karakan E, Sezer A (2021) Improved dataset for establishing novel relationships between compaction characteristics and physical properties of soils. Bull Eng Geol Env 80(11):8633–8663. https://doi.org/10.1007/s10064-021-02456-3

Shwan BJ (2023) Microstructural interpretation of effective stress equations for unsaturated sands. Geo-Engineering 14:4. https://doi.org/10.1186/s40703-022-00181-8

Silveira IA, Rodrigues RA (2020) Collapsible behavior of lateritic soil due to compacting conditions. Int J Civil Eng 18(10):1157–1166. https://doi.org/10.1007/s40999-020-00523-6

Won J, Ryu B, Choo H (2023) Evolution of maximum shear modulus and compression index of rigid–soft mixtures under repetitive K0 loading conditions. Acta Geotech 19(2):1–16. https://doi.org/10.1007/s11440-023-01945-x

Wu S, Gray DH, Richart FE Jr (1984) Capillary effects on dynamic modulus of sands and silts. J Geotech Eng 110(9):1188–1203. https://doi.org/10.1061/(asce)0733-9410(1984)110:9(1188)